DOI:
10.1021/acs.biochem.7b00157

Document Version
Peer reviewed version

Amyloid-like fibrils from an α-helical transmembrane protein

Karen Stroobants[a], Janet R. Kumita[a], Nicola J. Harris[b], Dimitri Y. Chirgadze[c], Christopher M. Dobson[a], Paula J. Booth[b] and Michele Vendruscolo[a*]

[a]*Department of Chemistry, University of Cambridge, Cambridge CB2 1EW, UK*

[b]*Department of Chemistry, King's College London, London SE1 1DB, UK*

[c]*Department of Biochemistry, University of Cambridge, Cambridge CB2 1GA, UK*

Keywords: membrane proteins, amyloid-like fibrils, protein misfolding, neurodegenerative disorders, protein aggregation

Corresponding Author:

Prof. Michele Vendruscolo

E-mail: mv245@cam.ac.uk.

Phone: +44 1223 763873

Abstract

The propensity to misfold and self-assemble into stable aggregates is increasingly recognised as a common feature of protein molecules. Our understanding of this phenomenon and of its links with human disease has increased substantially over the last two decades. Studies thus far, however, have been almost exclusively focussed on cytosolic proteins, resulting in a lack of detailed information about the misfolding and aggregation of membrane proteins. As a consequence, although such proteins make up approximately 30% of the human proteome and have high propensities to aggregate, relatively little is known about the biophysical nature of their assemblies. To shed light on this issue, we have studied as a model system an archetypical representative of the ubiquitous major facilitator superfamily, the *Escherichia coli* lactose permease (LacY). By using a combination of established indicators of cross-β structure and morphology, including the amyloid diagnostic dye thioflavin-T, circular dichroism, Fourier transform infrared spectroscopy, X-ray fibre diffraction, and transmission electron microscopy, we show that LacY can form amyloid-like fibrils under destabilising conditions. These results indicate that transmembrane α-helical proteins, as well as cytosolic proteins, have the ability to adopt this generic state.

Introduction

A wide range of medical conditions, including neurodegenerative disorders such as Alzheimer's and Parkinson's diseases, are associated with the misfolding and aggregation of specific proteins into amyloid fibrils[1-4]. *In vivo* and *in vitro* studies of these disease-related aggregates have led to the recognition of their common structural features, despite the diversity of the amino acid sequences and native state structures of the proteins by which they are formed[4]. In particular, it has been shown that amyloid fibrils possess a cross-β architecture, in which the β-strands that make up the β-sheets are orientated perpendicularly to the fibril axis[2, 4, 5]. As this fibrillar architecture can be adopted by a wide variety of different proteins[6-9], it has been suggested that polypeptide chains have a generic ability to form amyloid fibrils[4, 10].

Despite increasing evidence for the widespread nature of the amyloid phenomenon[3, 4, 6], little evidence has been obtained about this type of behaviour in the case of membrane proteins. This absence of information is particularly remarkable, as it is well known that the highly hydrophobic nature of membrane proteins makes them prone to self-association and aggregation under many conditions[11]. Indeed, hundreds of membrane proteins have been observed to aggregate upon ageing in *C. elegans*[12] and a set of genes found to be associated with human neurodegenerative disorders has been linked with membrane proteins involved in the oxidative phosphorylation pathway[13]. In addition, predictive models of protein homeostasis indicate that the aggregation propensity of membrane proteins is disproportionately high[14]. Moreover, the amyloid-β peptide (Aβ) associated with Alzheimer's disease, is a proteolytic fragment of the membrane protein APP[15], and the aggregation and formation of fibrils by fragments of luminal membrane protein domains has been reported[16].

Several reasons lie behind the current lack of detailed structural information about membrane protein aggregation, in particular the challenges inherent in their recombinant production and purification. These steps remain among the major

bottlenecks in many structural and functional analyses of these important biological components[17]. In contrast to the situation of cytosolic proteins, membrane proteins often require expression and purification procedures to be carried out in lipid or detergent environments[18]. Despite these difficulties, a more detailed knowledge of this group of proteins is absolutely essential for the understanding of normal and aberrant biological processes, as they represent about 30% of the human proteome[19] and comprise the vast majority of currently known drug targets[20].

Moreover, increased β-sheet structure has sparsely been reported for disease related membrane proteins. Perhaps the best studied of these proteins is the cystic fibrosis transmembrane conductance regulator (CFTR), an ABC transporter containing 12 transmembrane helices. Several mutations of this membrane protein result in a variety of cystic fibrosis phenotypes[21], spanning defects in synthesis, processing, trafficking, as well as functional deficits. Although most studies report a fast degradation of dysfunctional CFTR rather than formation of deposits[22], it has been indicated that misfolded aggregates with highly organized arrays of β-strands can form for the P205 mutant[23]. Retinitis pigmentosa, a progressive retinal degenerative disease, has been shown to be associated with mutations in rhodopsin, an α-helical membrane protein of the G-coupled protein receptor (GCPR) family[24]. Indeed, since the majority of these mutations result in the incorrect folding of the apoprotein opsin, retinitis pigmentosa has been classified as a protein misfolding disease[25, 26]. Despite the fact that misfolded opsin was initially presumed to form disordered aggregates in the endoplasmic reticulum (ER)[27], it has recently been shown that aggregates of the opsin variants G188R and P23H, formed in HEK293 cells, exhibit a high content of β-structure[28]. These appear to be distinct from amyloid fibrils since they do not enhance the fluorescence of ThT[28]. An increased tendency to form ordered β-sheet structure has also been reported for a model peptide with the partial sequence of a transmembrane domain of peripheral myelin protein 22 (PMP22)[29]. PMP22 is an α-helical transmembrane glycoprotein that is primarily expressed in Schwann cells, and its mutations are known to cause the peripheral neuropathy Charcot

Marie-Tooth disease[30]. Aggresome formation by this protein has been reported upon its overexpression in mice, although the structure of the protein within these aggregate-rich inclusions is not yet clear[31]. In addition, there is recent evidence for the formation of ThT-positive aggregates of the β-barrel transmembrane domain of the outer membrane protein A (OmpA) formed in the absence of lipid or lipid-mimetic membranes and in the presence of high concentrations of urea[32].

Overall, although increases in β-sheet structure have been reported in a number of cases[23, 28, 31, 32], it still remains unclear whether membrane proteins, like cytosolic proteins, have an inherent propensity to convert into amyloid fibrils. To address this problem, we have studied LacY, a representative of the major facilitator superfamily of transporters that are prevalent across prokaryotes and eukaryotes. The 417-residue protein is composed of 12 transmembrane α-helices arranged in two domains, with a substrate binding site at the domain interface[33]. Its crystal structure has been solved to 3.6 Å resolution[34] and its function has been studied in great detail[35]. The structure and *in vitro* folding of LacY have been studied both within micelles and liposomes[36-38]. These simple lipid-mimetic systems represent an ideal starting point for biophysical studies, and the relevance of their use is supported by extensive studies showing the tolerance of membrane proteins to changing lipid environments[39].

We should mention that, *in vivo*, LacY is translated directly into lipid membranes in *E. coli*, in the same way that most membrane proteins are directly translated into the ER membrane where they then reside[40]. Furthermore, a network of quality-control mechanisms has co-evolved with the biosynthesis and trafficking of membrane proteins in the ER, with the specific purpose to avoid their aggregation.[41] By contrast, in our *in vitro* study, we observe aggregation reactions in a convenient detergent system. Although these conditions are non-physiological, and our *in vitro* assays also lack the protein homeostasis controls present in the cellular environment, they enable us to explore the range of structural states accessible to LacY. Consistently, a number of experimental studies have already provided evidence of membrane protein aggregation within the cellular

environment. For example, even if in many proteomics studies membrane proteins tend to be discarded prior to analysis[42], several studies have reported the presence of membrane proteins in aggregates found in disease tissues. In particular, lysosomal ATPase and mitochondrial ATPase components have been found to co-aggregate in post-mortem amyloid plaques[43] and neurofibrillary tangles[44], respectively, and the accumulation of the Parkin-associated transmembrane receptor Pael-R in Lewy bodies has been reported[45]. These examples indicate that membrane proteins under stress can accumulate *in vivo* outside their native environments.

We report here the conversion of LacY into fibrillar aggregates with the characteristic features of the cross-β structure, and therefore demonstrate that an α-helical membrane protein can adopt a stable amyloid-like state analogous to those reported for cytosolic proteins.

Materials and Methods

Generation of the aggregation propensity profile of LacY

The CamSol method[46] was used to calculate the sequence-dependent intrinsic solubility of LacY, which we adopted as an indicator of its aggregation propensity, as both solubility and aggregation propensity describe the tendency of proteins to convert from the native state to insoluble aggregates. The CamSol method was derived by considering the physico-chemical properties of the amino acid sequences that are most responsible for their aggregation behaviour, including in particular the hydrophobic patterns, which tend to drive the aggregation process, and the presence of 'gatekeeper' residues (charged residues and prolines), which tend to prevent it[46]. The indication of α-helices and coil in the figure was based on the native structure of LacY[34, 47].

LacY Expression and Purification

LacY was purified as previously described[37] with modifications. LacY was expressed in One Shot BL21-AI chemically competent E. coli (Thermo Fisher Scientific, Paisley, UK), using the kanamycin resistant plasmid pET-28a. The cultures were grown at 37 °C in LB media and induced with 0.1% arabinose and 1 mM IPTG at an OD600 of 0.7–0.8 AU, and the cells were harvested by centrifugation (5000 X g, 45 min). Following growth and induction, the cells were lysed by three cycles in a high pressure homogenizer, and the membranes were sedimented by centrifugation (100,000 X g, 4 °C, 30 min) (Beck-man Coulter Ultracentrifuge, rotor 70Ti, High Wycombe, UK). The pellets were resuspended and incubated (4 °C, 2 h) in 25 ml solubilisation buffer [200 mM NaCl, 20 mM imidazole, 10 mM β-mercaptoethanol, 40 mM DDM and an EDTA free pro-tease inhibitor cocktail tablet (Roche Diagnostics Ltd, Burgess Hill, UK)]. The solubilised membranes were centrifuged (100,000 X g, 4 °C, 30 min), and the supernatans was retained for purification. For all steps of purification, the buffer contained 50 mM sodium phosphate (pH 7.4), 10% (v/v) glycerol, 10 mM β-mercaptoethanol and 1 mM DDM, with additional components indicated in brackets. Initial purification was per-formed with a 1 mL HisTrap HP Ni^{2+}-affinity column (GE Healthcare Ltd, Little Chalfont, UK), previously equilibrated with 10 column volumes (CV) of purification buffer (20 mM imidazole). Following loading of the sample, the column was washed with 5 CV of purification buffer (20 mM imidazole) and LacY was eluted with 50 CV of elution buffer (75 mM im-idazole). The eluted protein was transferred directly to a gel filtration column (SUP200 Superdex, GE Healthcare) to remove imidazole as well as multimeric protein species. The re-sulting protein fractions were analysed by SDS-PAGE using NuPAGE 4-12% gels with MES Buffer (Thermo Fisher Scien-tific) and UV-vis spectroscopy to verify the purity of the protein samples and determine their concentrations, respectively. The LacY concentration in the supernatant was determined from the absorbance at 280 nm, using ε_{LacY} = 76391 M^{-1} cm^{-1}. After purification, aliquoted samples were frozen in liquid N_2 and stored at -80 °C until use.

LacY Aggregation Procedure

LacY in 50 mM sodium phosphate 0.05% DDM pH 7.4 was used directly as obtained from the purification (2, 4 and occasionally 8 μM samples) or concentrated (to 8, 16 or 32 μM), and aggregation was initiated by increasing the temperature of the sample to 37 °C. When concentrating of the protein was required, Vivaspin20 concentrators with a 100 kDa cut-off (Millipore, Watford, UK) were used as these devices were reported to cause insignificant changes in the DDM concentration [(48, 49)]. The final DDM concentration was determined via colorimetric determination of the glycoside content [(49)]. The samples were continuously kept on ice or at 4 °C to minimize aggregate formation prior to any measurement. Concentrating the samples took approximately 35 minutes from defrosting. Samples were used immediately after concentrating, and were not refrozen.

ThT Fluorescence Assay

LacY (2, 4 and 8 μM as obtained after purification) in 50 mM sodium phosphate 0.05% DDM pH 7.4, was incubated at 37 °C in the presence of 4 μM of ultrapure ThT (Sigma-Aldrich, Dorset, UK). The change in the ThT fluorescence intensity (excitation at 440 nm, emission at 480 nm) was monitored over 48 h using a FLUOstar Optima plate reader (BMG Labtech, Aylesbury, UK) under quiescent conditions. Corning 96-well plates with half-area (black/clear bottom polystyrene) nonbinding surfaces (Fisher Scientific, Loughborough, UK) were used.

Analysis of LacY in the Supernatant

At the end of an aggregation experiment, the samples were centrifuged (15000 X g, 15 min), and the concentration of the free monomer was calculated by measuring the UV-vis spectrum of the supernatant. The same samples were analysed with SDS-PAGE. An aliquot of the LacY supernatant solution (15 μL) was mixed with NuPAGE LDS sample buffer (ThermoFisher Scientific) and 10 μL of the solution was run on a NuPAGE 4-12% Bis-Tris gel (ThermoFisher Scientific). A tricolor protein marker (Stratech Scientific, Suffolk, UK) was run in lane 4. The gel was stained with InstantBlue (Expedeon, Swavesey, UK).

Circular Dichroism Spectroscopy

A LacY solution (2 μM) in 50 mM phosphate buffer, 0.05% DDM, pH 7.4, before and after incubation at 37 °C for 48 h, was deposited in a circular cell. Far-UV CD spectra were recorded on an Aviv Circular Dichroism Spectrophotometer, Model 410 (Biomedical Inc., Lakewood, NJ, USA), with specially adapted sample detection (the detector is placed closer to the sample) to minimize scattering artefacts. Quartz circular cells were used, and CD spectra were obtained by averaging 2 to 5 individual spectra recorded between 260 nm and 190 nm at 0.5 nm interval with an averaging time of 2 s. For each protein sample, the CD signal of the buffer without protein was recorded and subtracted from the CD signal of each protein sample. The multiple scans were averaged and the buffer background was subtracted. The data were then converted from millidegrees to mean residue ellipticity[(50)].

Fourier Transform Infrared Spectroscopy

A LacY solution (concentrated to 16 μM) in 50 mM phosphate buffer, 0.05% DDM, pH 7.4, before and after incubation at 37 °C for 48 h, was deposited (10 μL) into a BioATR cell (Bruker Optics, Coventry, UK). FT-IR absorption spectra were collected in absorbance mode on an FT-IR Vertex 70 (Bruker) spectrometer fitted with BioATR cell (Bruker Optics, Coventry, UK). Spectra were corrected for the presence of sodium phosphate 50 mM, pH 7.4, 0.05% DDM. The secondary derivative for each spectrum was calculated using OriginPRO. In order to reduce the noise a FFT filter (10 pt) was initially applied, successively the curves were normalised and smoothed by a Savitski-Golay filter (9 pt).

Transmission Electron Microscopy

LacY solutions (concentrated to 16 μM) in 50 mM phosphate buffer, 0.05% DDM, pH 7.4, were incubated at 37 °C for 48 h and 5 μL of sample was applied to carbon-coated 400-mesh copper grids (EM Resolutions, Saffron Walden, UK). Samples were stained with 2% (w/v) uranyl acetate and imaged using a FEI Tecnai G_2 transmission electron microscope (Multi-Imaging Unit in the Department of Physiology, Development and Neuroscience, University of Cambridge, UK). Images

were analysed using the SIS Megaview II Image Capture system (Olympus).

X-ray Fibre Diffraction Pattern Analysis

LacY solutions (concentrated to 16 and 32 μM) in 50 mM phosphate buffer, 0.05% DDM, pH 7.4, were incubated at 37 °C for 48 h. The samples for fibre diffraction were dialysed against sodium phosphate 50 mM, pH 7.4, 0.05% DDM and a 5 μL aliquot was pipetted between wax stalks and left to dry. The experiments were performed at the Crystallographic X-ray Facility, Department of Biochemistry, University of Cambridge, UK. X-rays with a wavelength of 1.5418 Å were produced by a rotating copper anode MISCROSTAR generator (Bruker-AXS, Ltd), collimated and focused by HELIOS-MX high-brightness multilayer X-ray optics. Images were acquired on a PLATINUM135 CCD area detector (Bruker-AXS, Ltd Rigaku-MSC). The exposure time for the diffraction images was 60 s in each case. The diffraction pattern viewing and analysis was carried out using PORTEUM2 software package (reference: PROTEUM 2 User Manual, Bruker AXS, 2010).

Results and Discussion

LacY has a high intrinsic propensity for aggregation

In a preliminary assessment, we used the CamSol method[(46)] to calculate the sequence-dependent solubility of LacY (**Figure 1**), which is inversely related to the aggregation propensity score (see Material and Methods). As the native state of LacY comprises 12 transmembrane α-helices, the sequence may be expected to include highly hydrophobic and aggregation-prone regions outside its natural lipid environment, which are indeed present (red regions in the sequence profile in **Figure 1**).

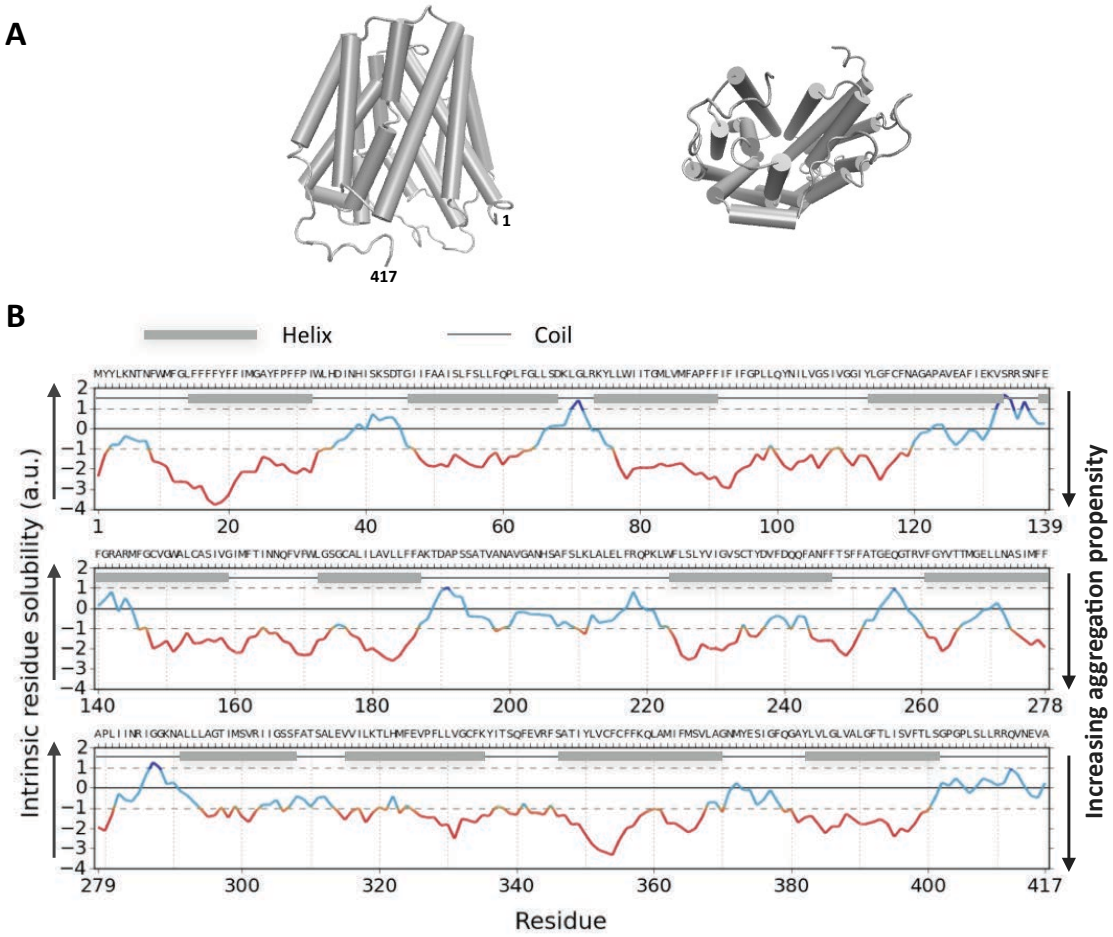

Figure 1. CamSol profile of LacY, as an indicator of its aggregation propensity. **(A)** Native structure of LacY (front and bottom view), which is shown for reference. The PDB structure 2V8N[34] was used to draw the cartoons, with cylinders representing α-helices and ribbons representing disordered coils. **(B)** CamSol[46] profile of LacY (see Materials and Methods). Regions denoted in red have a low intrinsic solubility and hence a high aggregation propensity. The positions of α-helices (as derived from[47]) are indicated by horizontal grey bars.

LacY readily forms aggregates at 37 °C and pH 7.4

LacY was expressed and purified into n-dodecyl β-d-maltoside (DDM) micelles according to standard procedures[37]. The detergent was used at a concentration of 1 mM (or 0.05%) in all experiments, which is well above its critical micelle concentration (CMC) of 0.16 mM[51]. Long chain maltoside detergents are generally used for LacY purification as they are well known to effectively maintain the

protein in solution[52]. In addition, it was established that LacY is stabilized by low temperature and glycerol[52], which was added in all purification buffers (in Materials and Methods). Despite these considerations, purification of LacY is challenging as the protein tends to aggregate readily at room temperature and even when kept on ice for few hours. Furthermore, as several biophysical techniques utilised in our studies require higher protein concentrations (at least in the range of 15-30 μM) than those initially obtained from the purification (typically in the range of 2-6 μM), the samples often required concentrating, thereby placing the protein under conditions where it is particularly vulnerable to aggregation prior to the start of any experiment. This aspect of the system made it difficult to characterise the precise starting point of the aggregation reaction, and consistently to avoid the presence of a small fraction of aggregated species at the initiation of the experiments.

In the experimental protocol described here, LacY (in 50 mM sodium phosphate pH 7.4, 0.05% DDM) was used as obtained from the purification procedure (2, 4 and 8 μM samples) or concentrated to 8, 16 or 32 μM. Amyloid-like structures often are observed under conditions that destabilize the protein under study[7], and as temperature increase in particular is know to destabilize LacY[52], aggregation of the protein was initiated by increasing the temperature of the sample from 4 °C to 37 °C. Visible precipitation of LacY in the micellar environment was observed after approximately 4 h for the 16 μM samples to approximately 8 h for the 2 μM samples, with increasing turbidity of the solutions at longer incubation times of up to 48 h. Aliquots taken at different time points during the incubation were centrifuged and the supernatant at each time point was analysed. The concentration of LacY in the supernatant at each time point was obtained from UV-vis spectra at 280 nm (**Table 1**) and observed to decrease gradually over time, resulting in less than 20% of the initial protein remaining in solution after 48 h of incubation. This ratio is consistent for the samples at higher concentrations. The same samples were analysed by SDS-PAGE (**Figure 2**) and the increasingly faint bands observed for the samples after increasing incubation times confirm the nearly complete conversion of the monomer into precipitating species after 48 h.

Table 1. LacY concentration in the supernatant over time. LacY solutions (2 μM) incubated in 50 mM phosphate buffer pH 7.4 with 0.05% DDM (37 °C, 48 h), were centrifuged after 0, 2, 4, 6, 24 and 48 h to precipitate the aggregated fraction, and the UV-vis signal at 280 nm of the remaining supernatant was monitored. The LacY concentration in the supernatant was determined from the absorbance at 280 nm, using ε_{LacY} = 76391 M^{-1} cm^{-1}. An average of two measurements from separate samples is shown (SD +/- 0.005 for A_{280}).

Time (h)	A_{280}	c (μM)
0	0.148	1.94
2	0.128	1.68
4	0.089	1.15
6	0.085	1.11
24	0.052	0.68
48	0.031	0.40

In the following sections, we describe a range of biophysical techniques that we have used to define the structural nature of the observed aggregates and to characterise their properties. Since near-complete precipitation of LacY from solution was observed after 48 h we did not extend experiments beyond this initial time frame.

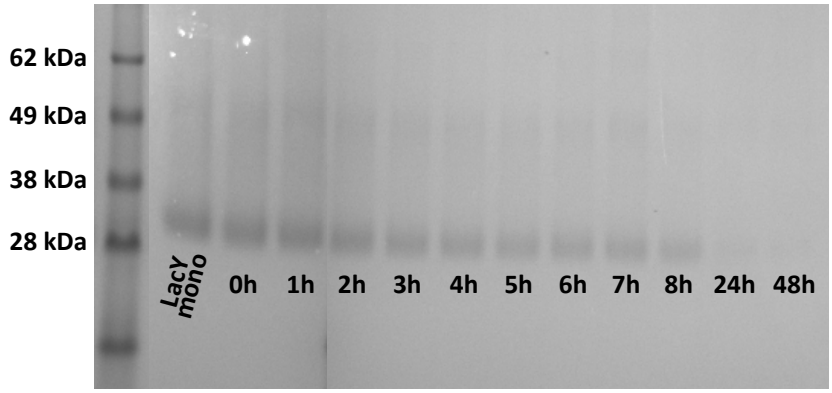

Figure 2. Fraction of LacY in the supernatant over time. LacY solutions (2 μM) incubated in 50 mM phosphate buffer pH 7.4 with 0.05% DDM (37 °C, 48 h), were centrifuged to precipitate the aggregated fraction and the remaining supernatant was analysed by SDS-PAGE gel after 0, 1, 2, 3, 4, 5, 6, 7, 8, 24 and 48 h (as indicated). LacY appears at ~28 kDa since it does not unfold in SDS and thus runs in its folded state (its expected MW is 48 kDa). The experiment was repeated twice; a representative data set is shown.

LacY aggregates are ThT positive

Amyloid-specific fluorescent dyes have been used for many years to identify amyloid assemblies[(1)] and *in vitro* assays involving these compounds remain a powerful approach to characterising amyloid-like fibrils and to monitoring the kinetics of their formation. One of the most widely used dyes is ThT, a positively charged benzothiazole salt that shows increased fluorescence upon interaction with amyloid fibrils[(53)]. Membrane proteins are highly hydrophobic in nature and could therefore adopt a different binding mode to ThT from cytosolic proteins. Although some studies have suggested that ThT binding to amyloid fibrils involves the formation of ThT micelles as a result of hydrophobic interactions[(54)], a model in which ThT specifically interacts with the cross-β strands that characterise the unique amyloid architecture is more widely accepted[(53)].

LacY solutions with concentrations of 2, 4 and 8 μM were incubated at 37 °C in the presence of 4 μM ThT, and the fluorescence signal was monitored over the course of 48 h. Within minutes, an increase in the fluorescence intensity at 480 nm was

observed, and sigmoidal aggregation curves were obtained by plotting the relative fluorescence intensities as a function of time (**Figure 3**). The initial high intensities, which were seen in all samples, are often observed in this type of kinetic experiments, and can be attributed to an equilibration at the higher temperature (from 4 °C to 37 °C in this case). Normalisation of the data shows an increase in the aggregation rate with increasing initial protein concentration (up to 8 μM – as these samples could be obtained directly after purification without the need for concentration) (**Figure 3B**). The ThT-positive character of the LacY aggregates provides a first indication that they may have a β-sheet rich amyloid-like nature. The enhanced fluorescence of ThT inside micelles, however, could be a result of electrostatic interactions with the charged detergent molecules[(55)]. Indeed, significant effects of this type have been observed for ThT simply in the presence of the anionic surfactant, sodium dodecyl sulphate (SDS), whereas relatively insignificant intensity changes were observed with neutral detergents such as Tween 20 and Triton-X-100[(55)]. Since DDM belongs to the latter category of detergents, only minor intensity changes were expected, and none were observed, in its presence (**Figure S1**). All spectra were corrected for potential buffer effects by monitoring the ThT fluorescence in sodium phosphate buffer containing equal DDM concentrations to those of the sample under investigation, showing that the increase in ThT fluorescence correlates with the presence of LacY aggregates as determined by centrifugation.

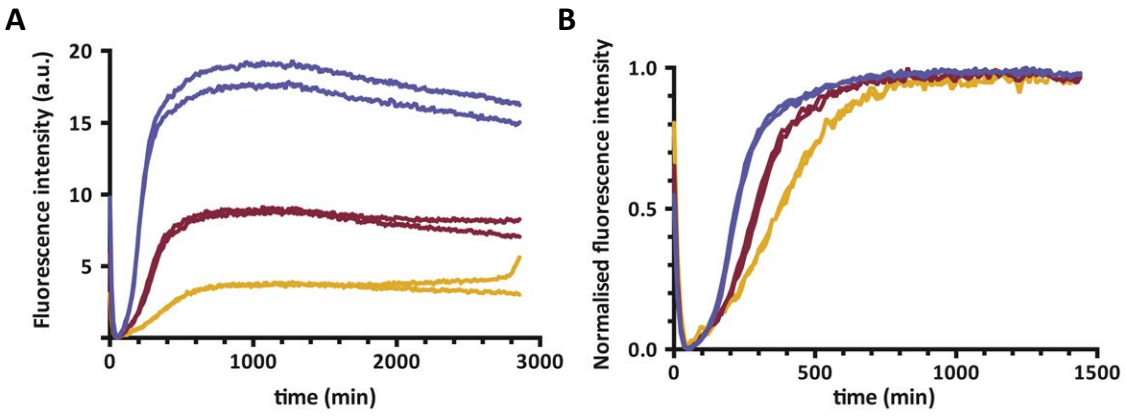

Figure 3. Enhancement of ThT fluorescence by LacY aggregates. (**A**) ThT fluorescence changes in monomer solutions of 2 µM (yellow), 4 µM (red) and 8 µM (blue) LacY (in duplicate) in 50 mM sodium phosphate pH 7.4 with 0.05% DDM. The solutions were incubated (37 °C, 48 h) in the presence of 4 µM ThT and the ThT fluorescence was continuously monitored. The fluorescence spectra were corrected for the signal in 50 mM sodium phosphate pH 7.4 with 0.05% DDM. (**B**) The spectra in panel (**A**) were normalised by subtracting the minimum, and dividing by the maximum fluorescence intensity for the respective data set. This procedure enables a straightforward comparison of the slopes of the intensity profiles for different concentrations. The experiment was repeated 5 times; a representative data set is presented.

LacY converts from α-helical to parallel β-sheet structure

In addition to monitoring dye-binding properties, direct detection of their characteristic β-sheet architecture is a key parameter in the identification of amyloid-like fibrils. Circular dichroism (CD) and Fourier transform infrared (FT/IR) spectroscopies are powerful techniques used to characterise protein secondary structure content and were used to monitor the changes in the LacY secondary structure upon aggregation[(56)]. The native LacY monomer has been studied extensively; an α-helical structure content of about 85% has been reported from CD measurements and is consistent with the crystal structure[(57)].

Aliquots from a LacY solution at a concentration of 2 µM were taken before and after incubation at 37 °C for 48 h, respectively, and CD spectra were recorded of

each sample (**Figure 4**). The spectrum of LacY as obtained from the purification and before incubation possesses characteristic minima at 208 and 223 nm, indicative of a highly α-helical structure, in accord with the LacY native fold[(57)]. The signal intensity was reduced significantly after incubation of the sample at 37 °C, indicating a loss of soluble protein. This result indicates that only soluble protein is being detected, while the aggregated fraction crashes out of solution and does not result in a detectable signal. Further secondary structure determination therefore was performed using FT/IR spectroscopy. This technique furthermore has a higher sensitivity and accuracy for resolving β-sheet compositions[(58-60)]. For example, whereas only changes in α-helical content were detectable by CD spectroscopy in the study of the secondary structure changes of opsin variants, changes in both α-helical and β-sheet content were observed for the same system using FT/IR spectroscopy[(28)]. As FT/IR requires higher protein concentrations than those obtained from the purification procedure, a concentrated sample was used for this analysis. The DDM concentration of the concentrated samples was verified via colorimetric determination of the glycoside content[(49)] and only small increases (from 0.050 to up to 0.057% **Table S1**) were detected. Aliquots from the LacY solution at a concentration of 16 μM were taken before and after incubation at 37 °C for 48 h, respectively, and FT/IR spectra were recorded of each sample (**Figure 5A**). The amide I / II regions of the spectra at both time points are shown, as well as the second derivative spectra (**Figure 5B**).

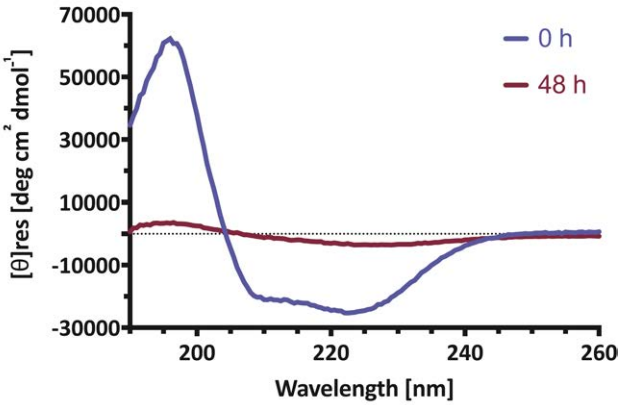

Figure 4. CD intensity decrease upon aggregation of LacY. LacY (2 µM) was incubated in 50 mM phosphate buffer pH 7.4 with 0.05% DDM, at 37 °C. CD spectra were recorded before (blue) and after 48 h of incubation (red). The spectra were corrected for 50 mM sodium phosphate pH 7.4 with 0.05% DDM. A minimum of 3 scans was averaged per time point. The experiment was repeated twice; a representative data set is presented.

The amide I band obtained for the LacY sample before incubation has its maximum at 1653 cm^{-1}, which is the characteristic region for α-helical/disordered structure content[61, 62]. This pre-incubation sample, although predominantly α-helical in nature, may contain some aggregated species due to its high protein concentration. After 48 h, the main peak is shifted to 1623 cm^{-1} where intermolecular β-sheet structure has its characteristic maximum[61]. The differences between β-sheet structure in amyloid-like fibrils compared to native states of proteins is evident from FT/IR data, with amyloid-like fibrils specifically populating the amide I region between 1610 and 1630 cm^{-1}[63]. A shift of the amide II band to lower wavelengths further reflects the formation of intermolecular hydrogen bonds upon incubation of the sample at 37 °C for 48 h. Deconvolution of the FT/IR data in **Figure 5A** indicates the conversion of mainly α-helical structure to 35% parallel β-sheet conformation after incubation at 37 °C for 48 h. In addition, the β-turn conformation (1682 cm^{-1}) and antiparallel β-sheet (1695 cm^{-1}) contents slightly increase upon incubation of the sample and these changes are intimately related with formation of cross-β sheet structure[63]. The FT/IR data thus indicate that the nature of the β-sheet fraction is typical of amyloid-like fibrils[63].

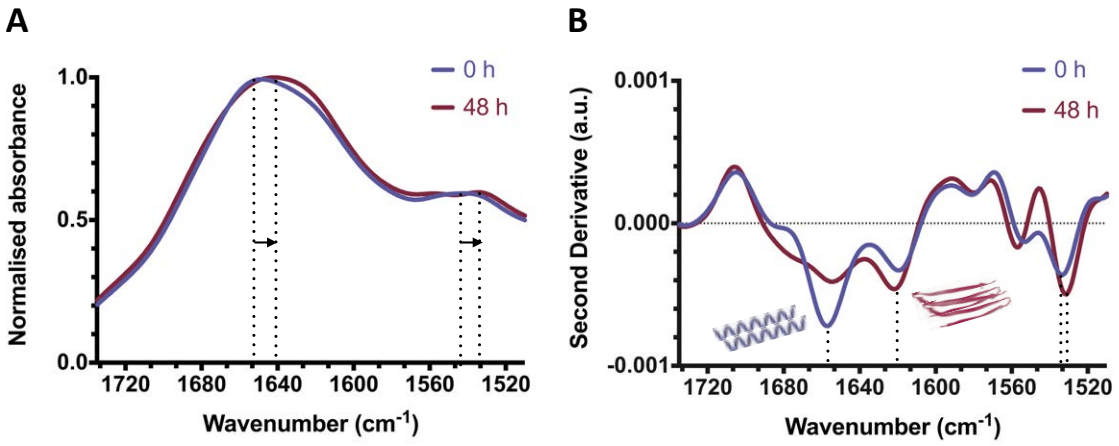

Figure 5. Secondary structure in LacY aggregates detected using FT/IR. (**A**) LacY (16 µM) was incubated in 50 mM phosphate buffer pH 7.4 with 0.05-0.06% DDM, at 37 °C. FT/IR spectra were recorded before (blue) and after 48 h of incubation (red) and corrected by subtracting the spectrum of the buffer solution. The dotted lines indicate the peak maxima, the arrows illustrate the peak shifts. A spectrum of LacY prior to concentration is not shown, since the protein directly obtained from the purification was not concentrated enough to result in a detectable spectrum. (**B**) The second derivative of the spectra before (blue) and after 48 h of incubation (red) show the appearance of peak positions in the amide I region at 1653 cm^{-1} and 1623 cm^{-1}, respectively. The dotted lines indicate the main peak minima. The experiment was repeated twice; a representative data set is presented.

Denaturant-resistant LacY aggregates have a fibrillar architecture

In light of the fibrillar nature of the aggregated samples indicated by the ThT assay and FT/IR data, we set out to obtain the corresponding fibre diffraction patterns. The diffraction patterns of the LacY sample after 48 h of incubation at 37 °C (**Figure 6A**) show a diffuse ring at a spacing between 4.5 and 4.8 Å and a very weak reflection at about 10 Å. While the observation of these reflections does confirm that fibrillar species are present, the weakness of the signal is a consequence of the low concentrations of fibrils and/or of a dilution effect due to the presence of less ordered species. In order to get more insights into the morphology of the species present in the LacY aggregates, transmission electron

microscopy (TEM) images were recorded for the incubated (at 37 °C for 48 h) LacY sample (concentrated at 16-32 μM). These measurements, although not of sufficient accuracy to reveal quantitative parameters such as width and height, showed that the aggregates have a fibrillar morphology, but are coated with less ordered material (**Figure 6C**), suggesting that the low resolution of the diffraction pattern is at least in part a consequence of dilution by disordered species.

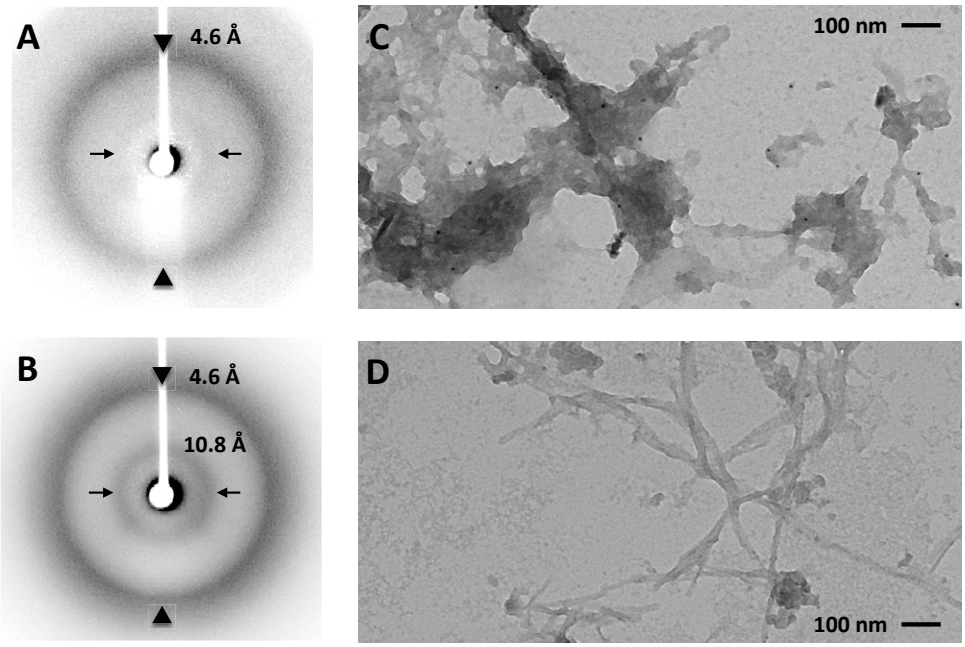

Figure 6. TEM and X-ray fibre diffraction data of LacY aggregates. (**A**) LacY (16-32 μM) was incubated in 50 mM phosphate buffer pH 7.4 with 0.05-0.06% DDM, at 37 °C. Fibre diffraction patterns from air-dried stalks of the samples were measured for the 48 h-incubated and (**B**) guanidinium hydrochloride treated samples. The arrowheads indicate the reflections at ca. 4.6 Å, while the arrows indicate the reflections at ca. 10.8 Å. (**C**) TEM grids were prepared for the same samples after 48 h of incubation, and (**D**) after 48 h of incubation followed by washing with 3 M guanidinium hydrochloride. These experiments were repeated 3 times, representative diffraction patterns and TEM images are shown.

To obtain more detailed images of the fibrillar species in the samples, we set out to separate the fibrillar and disordered components of the aggregates. Amyloid-like fibrils are typically extremely stable and considerably more resistant to relatively

high concentrations of denaturant than disordered aggregates[64]. We therefore incubated the aggregates in urea (8 M) or guanidinium hydrochloride (3 M) for 1 h, centrifuged the remaining insoluble material and re-examined it by TEM. The samples prepared in this manner show clearly the presence of substantially more homogeneous structures (**Figure 6D**), indicating that a denaturant-resistant fibrillar fraction can be isolated. Following treatment of the samples in urea (8 M) or guanidinium hydrochloride (3 M), the diffraction pattern was seen to be much more highly resolved as well (**Figure 6B**), showing reflections at 4.6 Å, characteristic of inter-strand spacing and at 10.8 Å, corresponding to the inter-sheet spacing as observed in amyloid fibrils[2]. The combination of these reflections is consistent with the cross-β pattern indicative of a β-sheet core structure, in which the constituent β-strands lie at right angles to the axis of the fibril. The characterised inter-strand and inter-sheet spacing, in combination with an extended degree of β-sheet content, enhanced ThT fluorescence emission and evidence for a fibrillar morphology indicate the ability of LacY to convert into amyloid-like fibrils *in vitro*.

Conclusions

The generality of the amyloid phenomenon has been firmly established for cytosolic proteins through a large number of case studies[1-8, 10]. By contrast, the extent of this phenomenon remains still rather unclear for membrane proteins, for which the conversion into β-sheet rich aggregates has been previously suggested[16, 23, 28, 31, 32], but only preliminary evidence for fibril formation so far has been provided[16, 23, 32]. In this work we have reported an extensive characterisation of the aggregates of LacY as amyloid-like fibrils. As many membrane proteins have sequences and overall architectures similar in nature to those of LacY, we anticipate that amyloid-like structures will be described in detail for a wider range of membrane proteins, and under a variety of conditions, thus enabling the biological relevance of these aggregates to be progressively defined.

Supporting Information

Table S1 indicating the DDM concentration of LacY samples after concentrating, and Figure S1 showing ThT intensity profiles for the DDM containing buffer in absence of the protein, are presented in the Supporting Information.

Funding Information

We are grateful for the award of the Marie Curie Career Development Fellowship (KS), as for support of this work by a Wellcome Trust Programme Grant 094425/Z/10/Z (CMD, MV).

Acknowledgements

The authors thank Prof. Kathryn Lilley and Drs. Daniel Nightingale of the Cambridge Centre for Proteomics for the use of the ultracentrifuge, Ewa Klimont for the help with setting up the membrane protein purification procedures in Cambridge, Francesco Simone Ruggeri for the help with the FT/IR deconvolution, and Lyn Carter and Jeremy Skepper of the Multi-Imaging Unit in the Department of Physiology, Development and Neuroscience, University of Cambridge, for the help with acquiring the TEM images. The X-ray fibre diffraction experiments were performed in the Crystallographic X-ray Facility (CXF) at the Department of Biochemistry, University of Cambridge (DYC).

Notes

The authors declare no competing financial interest.

References

1. Sipe, J. D., and Cohen, A. S. (2000). Review: History of the amyloid fibril, *J. Struct. Biol. 130*, 88-98.
2. Eisenberg, D., and Jucker, M. (2012) The amyloid state of proteins in human diseases, *Cell 148*, 1188-1203.
3. Knowles, T. P. J., Vendruscolo, M., and Dobson, C. M. (2014) The amyloid state and its association with protein misfolding diseases, *Nat. Rev. Mol. Cell Biol. 15*, 384-396.
4. Chiti, F., and Dobson, C. M. (2006) Protein misfolding, functional amyloid, and human disease, *Annu. Rev. Biochem. 75,* 333-366.
5. Sunde, M., Serpell, L. C., Bartlam, M., Fraser, P. E., Pepys, M. B., and Blake, C. C. F. (1997) Common core structure of amyloid fibrils by synchrotron X-ray diffraction, *J. Mol. Biol. 273*, 729-739.
6. Glenner, G. G., Eanes, E. D., Bladen, H. A., Linke, R. P., and Termine, J. D. (1974) Beta-pleated sheet fibrils - comparison of native amyloid with synthetic protein fibrils, *J. Histochem. Cytochem. 22*, 1141-1158.
7. Chiti, F., Webster, P., Taddei, N., Clark, A., Stefani, M., Ramponi, G., and Dobson, C. M. (1999) Designing conditions for in vitro formation of amyloid protofilaments and fibrils, *Proc. Natl. Acad. Sci. USA 96*, 3590-3594.
8. Fandrich, M., Fletcher, M. A., and Dobson, C. M. (2001) Amyloid fibrils from muscle myoglobin - Even an ordinary globular protein can assume a rogue guise if conditions are right, *Nature 410*, 165-166.
9. Guijarro, J. I., Sunde, M., Jones, J. A., Campbell, I. D., and Dobson, C. M. (1998) Amyloid fibril formation by an SH3 domain, *Proc. Natl. Acad. Sci. USA 95*, 4224-4228.
10. Dobson, C. M. (1999) Protein misfolding, evolution and disease, *Trends Biochem. Sci. 24*, 329-332.
11. Rath, A., and Deber, C. M. (2007) Membrane protein assembly patterns reflect selection for non-proliferative structures, *FEBS Lett. 581*, 1335-1341.
12. Walther, D. M., Kasturi, P., Zheng, M., Pinkert, S., Vecchi, G., Ciryam, P., Morimoto, R. I., Dobson, C. M., Vendruscolo, M., Mann, M., and Hartl, F. U.

(2015) Widespread proteome remodeling and aggregation in aging C-elegans, *Cell 161*, 919-932.

13. Ciryam, P., Kundra, R., Freer, R., Morimoto, R. I., Dobson, C. M., and Vendruscolo, M. (2016) A transcriptional signature of Alzheimer's disease is associated with a metastable subproteome at risk for aggregation, *Proc. Natl. Acad. Sci. USA 113*, 4753-4758.
14. Ciryam, P., Tartaglia, Gian G., Morimoto, Richard I., Dobson, Christopher M., and Vendruscolo, M. (2013) Widespread aggregation and neurodegenerative diseases are associated with supersaturated proteins, *Cell Rep. 5*, 781-790.
15. Kang, J., Lemaire, H. G., Unterbeck, A., Salbaum, J. M., Masters, C. L., Grzeschik, K. H., Multhaup, G., Beyreuther, K., and Mullerhill, B. (1987) The precursor of Alzheimers disease amyloid-a4 protein resembles a cell-surface receptor, *Nature 325*, 733-736.
16. Berson, J. F., Theos, A. C., Harper, D. C., Tenza, D., Raposo, G., and Marks, M. S. (2003) Proprotein convertase cleavage liberates a fibrillogenic fragment of a resident glycoprotein to initiate melanosome biogenesis, *J. Cell Biol. 161*, 521-533.
17. Wagner, S., Baars, L., Ytterberg, A. J., Klussmeier, A., Wagner, C. S., Nord, O., Nygren, P.-A., van Wijk, K. J., and de Gier, J.-W. (2007) Consequences of membrane protein overexpression in Escherichia coli, *Mol. Cell. Proteomics 6*, 1527-1550.
18. Harris, N. J., and Booth, P. J. (2012) Folding and stability of membrane transport proteins in vitro, *Biochim. Biophys. Acta 1818*, 1055-1066.
19. Krogh, A., Larsson, B., von Heijne, G., and Sonnhammer, E. L. L. (2001) Predicting transmembrane protein topology with a hidden Markov model: Application to complete genomes, *J. Mol. Biol. 305*, 567-580.
20. Overington, J. P., Al-Lazikani, B., and Hopkins, A. L. (2006) Opinion - How many drug targets are there?, *Nat. Rev. Drug Disc. 5*, 993-996.
21. Welsh, M. J., and Smith, A. E. (1993) Molecular mechanisms of CFTR chloride channel dysfunction in cystic fibrosis, *Cell 73*, 1251-1254.

22. Ward, C. L., Omura, S., and Kopito, R. R. (1995) Degradation of CFTR by the ubiquitin-proteasome pathway, *Cell 83*, 121-127.
23. Wigley, W. C., Corboy, M. J., Cutler, T. D., Thibodeau, P. H., Oldan, J., Lee, M. G., Rizo, J., Hunt, J. F., and Thomas, P. J. (2002) A protein sequence that can encode native structure by disfavoring alternate conformations, *Nat. Struct. Biol. 9*, 381-388.
24. Hartong, D. T., Berson, E. L., and Dryja, T. P. (2006) Retinitis pigmentosa, *Lancet 368*, 1795-1809.
25. Krebs, M. P., Holden, D. C., Joshi, P., Clark, C. L., III, Lee, A. H., and Kaushal, S. (2010) Molecular mechanisms of rhodopsin retinitis pigmentosa and the efficacy of pharmacological rescue, *J. Mol. Biol. 395*, 1063-1078.
26. Saliba, R. S., Munro, P. M. G., Luthert, P. J., and Cheetham, M. E. (2002) The cellular fate of mutant rhodopsin: quality control, degradation and aggresome formation, *J. Cell Sci. 115*, 2907-2918.
27. Surguchev, A., and Surguchov, A. (2010) Conformational diseases: Looking into the eyes, *Brain Res. Bull. 81*, 12-24.
28. Miller, L. M., Gragg, M., Kim, T. G., and Park, P. S. H. (2015) Misfolded opsin mutants display elevated beta-sheet structure, *FEBS Lett. 589*, 3119-3125.
29. Yamada, K., Sato, J., Oku, H., and Katakai, R. (2003) Conformation of the transmembrane domains in peripheral myelin protein 22. Part 1. Solution-phase synthesis and circular dichroism study of protected 17-residue partial peptides in the first putative transmembrane domain, *J. Peptide Res. 62*, 78-87.
30. Naef, R., and Suter, U. (1998) Many facets of the peripheral myelin protein PMP22 in myelination and disease, *Microsc. Res. Tech. 41*, 359-371.
31. Ryan, M. C., Shooter, E. M., and Notterpek, L. (2002) Aggresome formation in neuropathy models based on peripheral myelin protein 22 mutations, *Neurobiol. Disease 10*, 109-118.
32. Danoff, E. J., and Fleming, K. G. (2015) Aqueous, unfolded OmpA forms amyloid-like fibrils upon self-association, *PLoS One 10*, e0132301.

33. Abramson, J., Smirnova, I., Kasho, V., Verner, G., Kaback, H. R., and Iwata, S. (2003) Structure and mechanism of the lactose permease of *Escherichia coli*, *Science 301*, 610-615.
34. Guan, L., Mirza, O., Verner, G., Iwata, S., and Kaback, H. R. (2007) Structural determination of wild-type lactose permease, *Proc. Natl. Acad. Sci. USA 104*, 15294-15298.
35. Guan, L., and Kaback, H. R. (2006) Lessons from lactose permease, *Annu. Rev. Biophys. Biomol. Struct.*, *35*, 67-91.
36. Madej, M. G. (2014) Function, structure, and evolution of the Major Facilitator Superfamily: the LacY manifesto, *Adv. Biol. 2014*, 20.
37. Harris, N. J., Findlay, H. E., Simms, J., Liu, X., and Booth, P. J. (2014) Relative domain folding and stability of a membrane transport protein, *J. Mol. Biol. 426*, 1812-1825.
38. Findlay, H. E., and Booth, P. J. (2013) Folding alpha-helical membrane proteins into liposomes in vitro and determination of secondary structure, in *Membrane Proteins: Folding, Association, and Design*, 117-124.
39. Sanders, C. R., and Mittendorf, K. F. (2011) Tolerance to changes in membrane lipid composition as a selected trait of membrane proteins, *Biochemistry 50*, 7858-7867.
40. Alder, N. N., and Johnson, A. E. (2004) Cotranslational membrane protein biogenesis at the endoplasmic reticulum, *J. Biol. Chem. 279*, 22787-22790.
41. Vembar, S. S., and Brodsky, J. L. (2008) One step at a time: endoplasmic reticulum-associated degradation, *Nat. Rev. Mol. Cell Biol. 9*, 944-957.
42. Ibstedt, S., Sideri, T. C., Grant, C. M., and Tamas, M. J. (2014) Global analysis of protein aggregation in yeast during physiological conditions and arsenite stress, *Biol. Open 3*, 913-923.
43. Liao, L., Cheng, D., Wang, J., Duong, D. M., Losik, T. G., Gearing, M., Rees, H. D., Lah, J. J., Levey, A. I., and Peng, J. (2004) Proteomic characterization of postmortem amyloid plaques isolated by laser capture microdissection, *J. Biol. Chem. 279*, 37061-37068.
44. Sergeant, N., Wattez, A., Galvan-Valencia, M., Ghestem, A., David, J. P., Lemoine, J., Sautiere, P. E., Dachary, J., Mazat, J. P., Michalski, J. C., Velours, J.,

Mena-Lopez, R., and Delacourte, A. (2003) Association of ATP synthase alpha-chain with neurofibrillary degeneration in Alzheimer's disease, *Neuroscience 117*, 293-303.

45. Murakami, T., Shoji, M., Imai, Y., Inoue, H., Kawarabayashi, T., Matsubara, E., Harigaya, Y., Sasaki, A., Takahashi, R., and Abe, K. (2004) Pael-R is accumulated in Lewy bodies of Parkinson's disease, *Annals Neurol. 55*, 439-442.
46. Sormanni, P., Aprile, F. A., and Vendruscolo, M. (2015) The CamSol method of rational design of protein mutants with enhanced solubility, *J. Mol. Biol. 427*, 478-490.
47. Guan, L., Murphy, F. D., and Kaback, H. R. (2002) Surface-exposed positions in the transmembrane helices of the lactose permease of Escherichia coli determined by intermolecular thiol cross-linking, *Proc. Natl. Acad. Sci. USA 99*, 3475-3480.
48. Strop, P., and Brunger, A. T. (2005) Refractive index-based determination of detergent concentration and its application to the study of membrane proteins, *Protein Sci. 14*, 2207-2211.
49. Urbani, A., and Warne, T. (2005) A colorimetric determination for glycosidic and bile salt-based detergents: applications in membrane protein research, *Anal. Biochem. 336*, 117-124.
50. Kelly, S. M., Jess, T. J., and Price, N. C. (2005) How to study proteins by circular dichroism, *Biochim. Biophy. Acta 1751*, 119-139.
51. Kuhlbrandt, W. (1988) 3-Dimensional cystallization of membrane-proteins, *Q. Rev. Biophys. 21*, 429-477.
52. Engel, C. K., Chen, L., and Privé, G. G. (2002) Stability of the lactose permease in detergent solutions, *Biochim. Biophy. Acta 1564*, 47-56.
53. Biancalana, M., and Koide, S. (2010) Molecular mechanism of Thioflavin-T binding to amyloid fibrils, *Biochim. Biophy. Acta 1804*, 1405-1412.
54. Khurana, R., Coleman, C., Ionescu-Zanetti, C., Carter, S. A., Krishna, V., Grover, R. K., Roy, R., and Singh, S. (2005) Mechanism of thioflavin T binding to amyloid fibrils, *J. Struct. Biol. 151*, 229-238.

55. Kumar, S., Singh, A. K., Krishnamoorthy, G., and Swaminathan, R. (2008) Thioflavin T displays enhanced fluorescence selectively inside anionic micelles and mammalian cells, *J. Fluoresc. 18*, 1199-1205.

56. Bouchard, M., Zurdo, J., Nettleton, E. J., Dobson, C. M., and Robinson, C. V. (2000) Formation of insulin amyloid fibrils followed by FTIR simultaneously with CD and electron microscopy, *Protein Sci. 9*, 1960-1967.

57. Foster, D. L., Boublik, M., and Kaback, H. R. (1983) Structure of the lac carrier protein of Escherichia-coli, *J. Biol. Chem. 258*, 31-34.

58. Uversky, V. N., Li, J., and Fink, A. L. (2001) Evidence for a partially folded intermediate in alpha-synuclein fibril formation, *J. Biol. Chem. 276*, 10737-10744.

59. Barth, A., and Zscherp, C. (2002) What vibrations tell us about proteins, *Q. Rev. Biophys. 35*, 369-430.

60. Calero, M., and Gasset, M. (2012) Featuring amyloids with fourier transform infrared and circular dichroism spectroscopies, in *Amyloid Proteins: Methods and Protocols*, 53-68.

61. Krimm, S., and Bandekar, J. (1986) Vibrational spectroscopy and conformation of peptides, polypeptides, and proteins, *Adv. Prot. Chem. 38*, 181-364.

62. Arrondo, J. L. R., Muga, A., Castresana, J., and Goni, F. M. (1993) Quantitative studies of the structure of proteins in solution by fourier-transform infrared-spectroscopy, *Prog. Biophys. Mol. Biol. 59*, 23-56.

63. Zandomeneghi, G., Krebs, M. R. H., McCammon, M. G., and Fandrich, M. (2004) FTIR reveals structural differences between native beta-sheet proteins and amyloid fibrils, *Protein Sci. 13*, 3314-3321.

64. Baldwin, A. J., Knowles, T. P. J., Tartaglia, G. G., Fitzpatrick, A. W., Devlin, G. L., Shammas, S. L., Waudby, C. A., Mossuto, M. F., Meehan, S., Gras, S. L., Christodoulou, J., Anthony-Cahill, S. J., Barker, P. D., Vendruscolo, M., and Dobson, C. M. (2011) Metastability of native proteins and the phenomenon of amyloid formation, *J. Am. Chem. Soc. 133*, 14160-14163.

For Table of Contents Use Only

Amyloid-like fibrils from an α-helical transmembrane protein

Karen Stroobants, Janet R. Kumita, Nicola J. Harris, Dimitri Y. Chirgadze, Christopher M. Dobson, Paula J. Booth and Michele Vendruscolo